

Immunity Of AC–DC Harmonics In VSC HVDC Transmission For Multi-Level Converters

Surya Manoj Vuddagiri
Assistant Professor

K Kiran Kumar
Assistant Professor

Abstract

They are very attractive techniques for the voltage-source-converter-(VSC) based high-voltage dc (HVDC) power transmission systems. The paper discusses optimized modulation patterns which offer controlled harmonic immunity between the ac and dc side. This method based on selective harmonic elimination pulse-width modulation (SHE-PWM) which offer the lowest possible number of switching transitions. This feature also results in the lowest possible level of converter switching losses. The application focuses on the three-level converter when its dc-link voltage contains a mix of low-frequency harmonic components. Simulation results are presented to confirm the validity of the proposed switching patterns.

1. Introduction

The continuous growth of electricity demand and ever increasing society awareness of climate change issues directly affect the development of the electricity grid infrastructure. The utility industry faces continuous pressure to transform the way the electricity grid is managed and operated. On one hand, the diversity of supply aims to increase the energy mix and accommodate more and various sustainable energy sources. On the other hand, there is a clear need to improve the efficiency, reliability, energy security, and quality of supply. With the breadth of benefits that the smart grid can deliver, the improvements in technology capabilities, and the reduction in technology cost, investing in smart grid technologies has become a serious focus for utilities [1].

Advanced technologies, such as flexible alternating current transmission system (FACTS) and voltage-source converter (VSC)-based high-voltage dc (HVDC) power transmission systems, are essential for the restructuring of the power systems into more automated, electronically controlled smart grids. The most important control and modelling methods of VSC-based HVDC systems and the list of existing installations are available in [2].

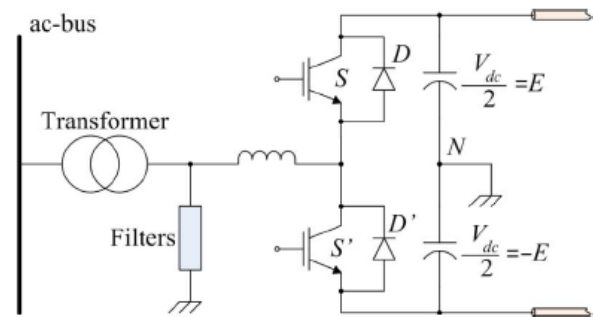


Fig. 1. Phase of the two-level VSC for the HVDC power transmission system.

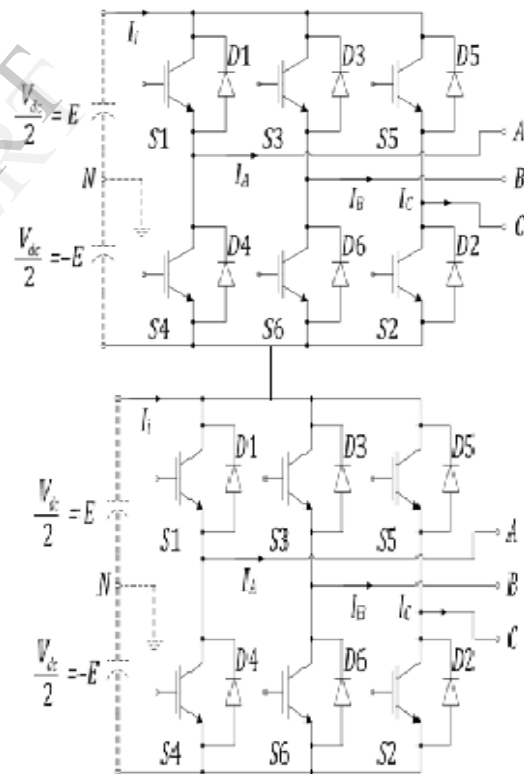


Fig. 2. Three-phase three-level VSC.

The first generation of utility power converters is based on current-source converter (CSC) topologies [3], [4]. Today, many projects still use CSCs due to their ultra-high power capabilities. With the invention of fully controlled power semiconductors, such as insulated-gate bipolar transistors (IGBTs) and integrated gate-commutated thyristors (IGCTs), the VSC

topologies are more attractive due to their four-quadrant power-flow characteristics. A typical configuration of the VSC-based HVDC power transmission system is shown in Fig. 1 as it is shown in [7] and [8].

Multilevel converters [2] can be more efficient but they are less reliable due to the higher number of components and the complexity of their control and construction. Increasing the number of levels above three is a difficult task for the industry. The multilevel converters are beyond the scope of this paper. This paper focuses on the three-phase three-level VSC topology (Fig. 2) and associated optimized modulation.

In most cases, the voltage of the dc side of the converter is assumed to be constant and the ac network is assumed to be balanced. However, fluctuations at various frequencies often occur on the dc side which usually appear as harmonics of the ac-side operating frequency. The most significant harmonic introduced to the dc-side voltage spectrum by an unbalanced three-phase ac-network is the 2nd harmonic. Inverters with 2nd harmonic on the dc bus generate the third harmonic on the ac side [10]. The proposed M-type modulation technique allows 33% reduction in the switching transitions without lowering the order of the predominant harmonic. The geometrical technique of [12] proposes a numerical calculation by modifying the pulse-width to cancel the harmonics produced by the dc-side ripple voltage. It has lower total harmonic distortion (THD) when compared with the conventional triangular sinusoidal PWM in the case where the dc-link voltage also fluctuates. However, [11] and [12] deal with sinusoidal-PWM techniques, which require a relatively high number of transitions per cycle to eliminate the low-order harmonics. Selective harmonic elimination pulse-width modulation (SHE-PWM) is the harmonic control with the lowest possible switching to give tightly controlled voltage spectrum and increase the bandwidth between the fundamental frequency and the first significant harmonic.

In the last decade or so, the size and level of power handling capability of the VSCs has increased substantially and has reached new heights for utility applications. As the interaction between the dc and ac systems increases and the power handling capability of these converters increases, it is important to further understand and study the effects of voltage and current harmonics on the converter design and operation and system performance. Any measures to minimize or even eliminate such unnecessary flowing of harmonics between the two systems (i.e., the ac and dc) are beneficial.

For instance, an approach that determines the harmonic Spectrum of the dc-bus currents of VSCs is presented in [14]. For a two-level three-phase

VSC, a general method for calculating the dc-bus currents for unbalanced, balanced, linear, and nonlinear loads is described in [15]. However, even if the converters have less dc-side ripple voltage with smaller dc-link capacitors than conventional methods, the capacitors remain one of the components most prone to failure. Minimizing or eliminating harmonic flows in the dc-link capacitors will decrease the dissipated heat and increase overall reliability and efficiency.

On the other hand, optimized modulation methods offer many advantages toward tight control of converter-generated harmonics [19]. A minimization method to find the complete set of solutions by solving the SHE-PWM equations for two-level inverters is discussed in [20]. In this paper, the dc-link voltage is assumed to be constant. In [10], a method is proposed to prevent the dc-link ripple voltage from creating low-order harmonics on the ac side of fixed and variable frequency inverters. However, only one of the multiple SHE-PWM sets [20] of solutions is reported.

An investigation of the harmonic interaction between the ac and dc side for STATCOM is presented in [21] including the so-called dynamic SHE-PWM scheme based on pre-calculated angles for better THD. However, the dynamic SHE-PWM scheme is applied only for a three-level converter and can be applied only for known magnitude and frequency of the ripple. However, only one set of SHE-PWM solutions is considered which requires the exact values of magnitude, phase, and frequency of the ripple in order to be implemented.

Control strategies to compensate unbalances are reported in the literature. Mild imbalances caused by unbalanced loads of the ac side are regulated by using separate control loops for the positive- and negative-sequence components of the voltage as proposed in [23]. Efficient control of unbalanced compensator currents can be achieved by a control algorithm based on the D-STATCOM model [24]. D-STATCOM allows separate control of positive- and negative-sequence currents and decoupled current control of the $d-q$ frame. An advanced strategy based on direct power control under unbalanced grid voltage conditions has been recently presented for a doubly fed induction generator [25]. To take the full advantages of VSCs for HVDC power transmission systems, an auxiliary controller is added to the main controller which is conventionally implemented in the positive-sequence - frame. To compensate for unbalanced ac-side loads, the auxiliary controller is implemented in the negative-sequence - frame.

The objective of this paper is to discuss the effectiveness of optimized modulation based on pre-calculated SHE-PWM in a three-level three-phase VSC to make the ac side immune from the fluctuations of the dc link without the use of

passive components. However, since the VSC studied here does not include a closed-loop controller, strategies to compensate unbalances are not addressed in this paper.

This paper is organized in the following way. In Section II, a brief analysis of the VSC and the modulation method is provided. Section III contains the characteristics of the method on a VSC with dc-side ripple voltage. Section IV provides extensive experimental results to support the theoretical arguments. Conclusions are documented in Section V.

2. Analysis of the PWM Converter and SHE-PWM

The optimized SHE-PWM technique is investigated on a three-level three-phase VSC topology with IGBT technology, shown in Fig. 2. A typical periodic three-level SHE-PWM waveform is shown in Fig. 3.

The waveforms of the line-to-neutral voltages can be expressed as follows:

$$V_{LN} = \begin{bmatrix} V_{AN} \\ V_{BN} \\ V_{CN} \end{bmatrix} = V_{dc} \begin{bmatrix} \sum_{n=1}^{\infty} A_n \sin n\omega_o t \\ \sum_{n=1}^{\infty} A_n \sin n(\omega_o t - \frac{2\pi}{3}) \\ \sum_{n=1}^{\infty} A_n \sin n(\omega_o t + \frac{2\pi}{3}) \end{bmatrix} \quad (1)$$

Where ω_o is the operating frequency of the ac, and V_{dc} is dc-link voltage.

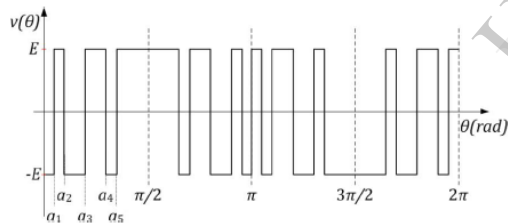


Fig. 3. Typical three-level PWM switching waveform with five angles per quarter cycle.

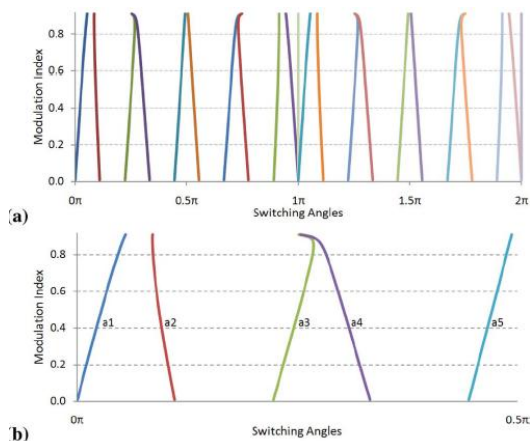


Fig. 4. Solution trajectories. (a) Per-unit modulation index over a complete periodic cycle. (b) Five angles in radians.

Thus, the line-to-line voltages are given by

$$V_{LL} = \begin{bmatrix} V_{AB} \\ V_{BC} \\ V_{CA} \end{bmatrix} = \sqrt{3} \cdot V_{dc} \begin{bmatrix} \sum_{n=1}^{\infty} A_n \sin n(\omega_o t + \frac{\pi}{6}) \\ \sum_{n=1}^{\infty} A_n \sin n(\omega_o t - \frac{\pi}{2}) \\ \sum_{n=1}^{\infty} A_n \sin n(\omega_o t + \frac{5\pi}{6}) \end{bmatrix} \quad \dots (2)$$

The SHE-PWM method offers numerical solutions which are calculated through the Fourier series expansion of the waveform

$$M = 1 + 2 \sum_{i=1,2,3\dots}^{N+1} (-1)^i \cos(\alpha_i)$$

$$0 = 1 + 2 \sum_{i=1,2,3\dots}^{N+1} (-1)^i \cos(k\alpha_i) \quad \dots (3)$$

Where $N+1$ are the angles that need to be found.

Using five switching angles per quarter-wave ($N=4$) SHE-PWM, $k=5, 7, 11, 13$ to eliminate the 5th, 7th, 11th, and 13th harmonics. During the case of a balanced load, the third and all other harmonics that are multiples of three are cancelled, due to the 120 symmetry of the switching function of the three-phase converter. The even harmonics are cancelled due to the half-wave quarter-wave symmetry of the angles, being constrained by $0 < \alpha_1 < \alpha_2 < \dots < \alpha_{N+1} < \pi/2$

3. Ripple Repositioning Technique

In this section, the technique to reposition the low-order harmonics produced by the dc-link ripple voltage of a VSC is described. The switching angles are pre-calculated for every available modulation index (M) to obtain the trajectories for the SHE-PWM, as shown in Fig. 4.

The intersections of the trajectories shown in Fig. 4 with any horizontal straight line, called the modulating signal (M_s) (i.e., an imaginary line of $M=0.75$ p.u.), give the switching angles of the specific modulation index. Those switching angles are identical to the solution of the conventional SHE-PWM method, so when the dc bus voltage is constant, all harmonics before the 17th one are eliminated. However, when the dc bus voltage is fluctuating, other harmonics are introduced. When the dc link has a ripple voltage of constant frequency ω_r and amplitude k times the dc-side voltage, the line-to-neutral voltage is represented as

$$V_{LN} = V_{LN} (1 + k \sin \omega_r t) \quad \dots (4)$$

Therefore, the modified line-to-line voltage of (2) becomes

$$\begin{aligned}
 V'_{AB} &= V_{AB} (1 - k \sin \omega_r t) \\
 &= \sqrt{3} \cdot V_{dc} \sum_{n=1}^{\infty} \left\{ A_n \sin n \left(\omega_o t + \frac{\pi}{6} \right) \right. \\
 &\quad \left. + \frac{k}{2} A_n \cos \left[(\omega_r - n\omega_o) t - n \frac{\pi}{6} \right] \right. \\
 &\quad \left. - \frac{k}{2} A_n \cos \left[(\omega_r + n\omega_o) t + n \frac{\pi}{6} \right] \right\}
 \end{aligned}
 \quad \text{--- (5)}$$

The method is used in the same way as in (5) to derive the other two line-to-line voltages of the three-phase converter: V'_{BC} and V'_{CA} . As was already mentioned, unbalance on the ac network can cause the 2nd harmonic on the dc-side voltage. Hence, $\omega_r = 2\omega_o$, and by substituting $n=1$ in (5), the lower order harmonics are given by

$$\begin{aligned}
 V_{h1} &= \frac{\sqrt{3}}{2} V_{dc} A_1 k \cos \left(\omega_o t - \frac{\pi}{6} \right) \\
 V_{h2} &= \frac{\sqrt{3}}{2} V_{dc} A_1 k \cos \left(3\omega_o t + \frac{\pi}{6} \right).
 \end{aligned}
 \quad \text{--- (6)}$$

The negative-sequence fundamental component and the positive-sequence 3rd harmonic are created on the ac side since it is proven in (6). For a constant dc-bus voltage, the modulating signal is a straight line of magnitude equal to the modulation index. For the fluctuating dc-bus voltage, the modulating signal is divided by, $(1+k \sin \omega_r t)$ which is the sum of the average per-unit value of the dc link and the ripple voltage in order to satisfy the repositioning technique. So when the magnitude of the dc-link voltage is instantaneously increased by a certain amount, the modulating signal's amplitude is reduced by using the switching angles of a lower modulation index. Therefore, by using the higher modulation index at the instants that the voltage is reduced and lower modulation index at the instants that the voltage is increased, the amount of ripple is reversed.

According to Fourier transform properties, multiplication in one domain corresponds to convolution in the other domain. So even if one frequency is removed from the modulated signal, it is expected to appear as sidebands of the switching frequency. SW is the switching function of the conventional SHE-PWM and the new switching function is represented by

$$SW' = \frac{1}{1 + k \sin \omega_r t} \cdot SW.$$

Therefore, the relevant line-to-neutral voltage is given by

$$V'_{LN} = V_{dc} (1 + k \sin \omega_r t) \cdot SW'.$$

The new switching function has the property of nullifying the low-order harmonics of the ac side, produced by the ripple of the dc-side voltage. This new switching function is generated from the respective intersections of the modified

modulating signal and the trajectories of harmonic elimination solutions.

3.1 Simulation Result

The MATLAB/SIMULINK software is used to demonstrate the dc-link ripple-voltage repositioning technique. Key results are presented in Figs. 5–7. Fig. 5 shows the simulation results of the method for the case that the dc-bus voltage has no ripple. The modulating signal is equal to the modulation index since the dc-link voltage is constant. Hence, the results are identical to the ones taken by using conventional SHE-PWM with a fixed modulation index (i.e, $M_s = M = 0.75$).

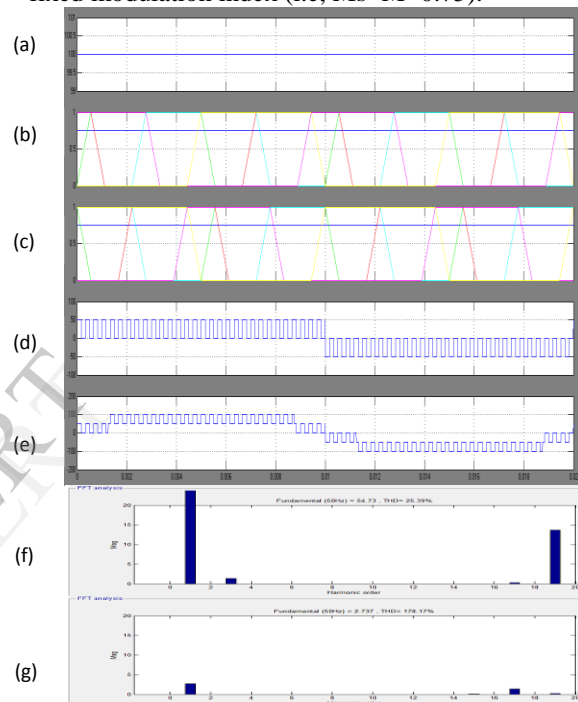


Fig. 5. Simulation results for SHE-PWM (a) DC-link voltage. (b) and (c) Solution trajectories to eliminate harmonics and intersection points with the modulating signal ($M = 0.75$). (d) Line-to-neutral voltage. (e) Line-to-line voltage. (f) and (g) Positive- and negative-sequence line-to-line voltage spectra, respectively.

Fig. 6 shows what happens when 10% of 2nd harmonic is added to the dc-link voltage. The switching angles are unchanged but the amplitude of the output voltage is fluctuating. The modulating signal is forced to be constant to give the same results with the conventional SHE-PWM. The value of the fundamental component is increased by 5% and a value of the 3rd harmonic is equal to 5% of the fundamental that appears in the spectrum of Fig. 6(f).

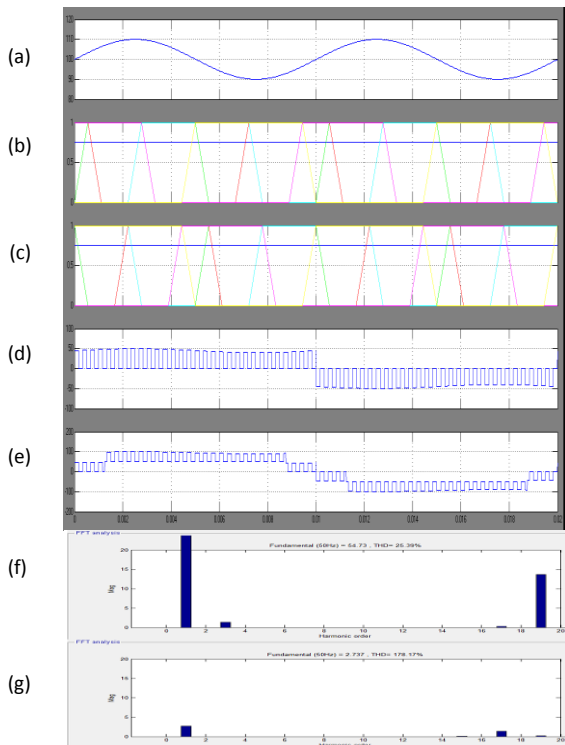


Fig. 6. Simulation results for SHE-PWM (a) DC-link voltage. (b) and (c) Solution trajectories to eliminate harmonics and intersection points with the modulating signal ($M = 0.75$). (d) Line-to-neutral voltage. (e) Line-to-line voltage. (f) and (g) Positive- and negative-sequence line-to-line voltage spectra, respectively.

By applying the dc-link ripple-voltage repositioning (Fig. 7), it is observed that the switching angles have slightly shifted. As shown in Fig. 7(f), the value of the fundamental component is equal to the one of Fig. 5(f). The 3rd harmonic no longer exists.

The modulating signal can be represented by the equation

$$M_s = \frac{M \cdot V_{dc \text{ mean}}}{V_{dc \text{ real}}}$$

Where $V_{dc \text{ mean}}$ is the average value of the dc-link voltage and $V_{dc \text{ real}}$ is the online dc-link voltage with 2nd harmonic ripple voltage on the dc bus, both per unit

Conclusion

An optimized SHE-PWM technique, which offers immunity between the ac and dc side in a three-level three-phase VSC, is discussed in this paper. The technique is highly significant in HVDCs due to the elimination of every low-order harmonic of the ac side produced by the dc-link ripple voltage.

The dc-link ripple repositioning technique regulates the magnitude of the fundamental component and eliminates the low-order harmonics of the ac side even when the dc bus voltage fluctuates.

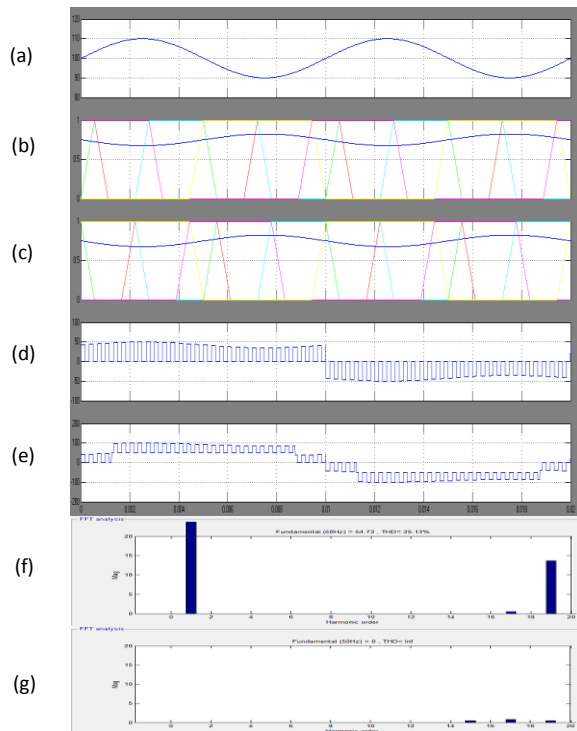


Fig. 7. Simulation results for 10% ripple of the 2nd harmonic at the dc bus by using the repositioning technique. (a) DC-link voltage with 10% ripple. (b) and (c) Modified modulating function and its intersection with the solution trajectories. (d) Line-to-neutral voltage. (e) Line-to-line voltage. (f) and (g) Positive- and negative-sequence line-to-line voltage spectra, respectively.

This is an online method which can be applied for eliminating any low-order harmonic frequency regardless of amplitude or phase shift of the ripple. There are some limitations related to the maximum modulation index available for SHE-PWM angles.

The repositioning technique also causes a reflection with respect to the midpoint between the fundamental component and the first significant harmonic. On the other hand, it eliminates all low-order ac-side harmonics for every dc-bus ripple voltage of frequency below the midpoint harmonic.

References

- [1] J. McDonald, "Leader or follower [The business scene]," IEEE Power Energy Mag., vol. 6, no. 6, pp. 18–90, Nov. 2008.
- [2] N. Flourentzou, V. G. Agelidis, and G. D. Demetriades, "VSC-based HVDC power transmission systems: An overview," IEEE Trans. Power Electron., vol. 24, no. 3, pp. 592–602, Mar. 2009.
- [3] A. A. Edris, S. Zelingher, L. Gyugyi, and L. J. Kovalsky, "Squeezing more power from the grid," IEEE Power Eng. Rev., vol. 22, no. 6, pp. 4–6, Jun. 2002.
- [4] B. K. Perkins and M. R. Iravani, "Dynamic modeling of high power static switching circuits in the dq-frame," IEEE Trans. Power Syst., vol.14, no. 2, pp. 678–684, May 1999.
- [5] J. Arrillaga, Y. H. Liu, and N. R. Watson, Flexible

Power Transmission: The HVDC options. Hoboken, NJ: Wiley, 2007.

[6] G. Asplund, "Application of HVDC light to power system enhancement," in Proc. IEEE Power Eng. Soc. Winter Meeting, Singapore, Jan. 2000, vol. 4, pp. 2498–2503.

[7] P. N. Enjeti and W. Shireen, "A new technique to reject dc-link voltage ripple for inverters operating on programmed PWM waveforms," IEEE Trans. Power Electron., vol. 7, no. 1, pp. 171–180, Jan. 1992.

[8] J. Y. Lee and Y. Y. Sun, "Adaptive harmonic control in PWM inverters with fluctuating input voltage," IEEE Trans. Ind. Electron., vol. IE-33, no. 1, pp. 92–98, Feb. 1986.

[9] S. Funabiki and Y. Sawada, "Computative decision of pulse width in three-phase PWM inverter," in Proc. IEEE Industry Applications Soc. Annu. Meet., Pittsburgh, PA, Oct. 1988, pp. 694–699.

[10] B. P. McGrath and D. G. Holmes, "A general analytical method for calculating inverter dc-link current harmonics," in Proc. IEEE Ind. Appl. Soc. Annu. Meeting, Edmonton, AB, Canada, Oct. 2008, pp. 1–8.

[11] A. M. Cross, P. D. Evans, and A. J. Forsyth, "DC link current in PWM inverters with unbalanced and nonlinear loads," Proc. Inst. Elect. Eng., Elect. Power Appl., vol. 146, no. 6, pp. 620–626, Nov. 1999.

[12] P. N. Enjeti, P. D. Ziogas, and J. F. Lindsay, "Programmed PWM techniques to eliminate harmonics: A critical evaluation," IEEE Trans. Ind. Appl., vol. 26, no. 2, pp. 302–316, Mar. 1990.

[13] V. G. Agelidis, A. Balouktsis, I. Balouktsis, and C. Cossar, "Multiple sets of solutions for harmonic elimination PWM bipolar waveforms: Analysis and experimental verification," IEEE Trans. Power Electron., vol. 21, no. 2, pp. 415–421, Mar. 2006.

[14] L. Ran, L. Holdsworth, and G. A. Putrus, "Dynamic selective harmonic elimination of a three-level inverter used for static VAR compensation," Proc. Inst. Elect. Eng., Gen., Transm. Distrib., vol. 149, no. 1, pp. 83–89, Jan. 2002.

[15] C. Hochgraf and R. H. Lasseter, "Statcom controls for operation with unbalanced voltages," IEEE Trans. Power Del., vol. 13, no. 2, pp. 538–544, Apr. 1998.

[16] D. Santos-Martin, J. L. Rodriguez-Amenedo, and S. Arnalte, "Direct power control applied to doubly fed induction generator under unbalanced grid voltage conditions," IEEE Trans. Power Electron., vol. 23, no. 5, pp. 2328–2336, Sep. 2008.